PHYSICAL REVIEW B VOLUME 22, NUMBER 6 15 SEPTEMBER 1980

Site effect on the impurity levels in 4*H*, 6*H*, and 15*R* SiC

M. Ikeda, H. Matsunami, and T. Tanaka*

Department of Electronics, Faculty of Engineering, Kyoto University, Kyoto 606, Japan

(Received 31 December 1979)

The existence of site-dependent impurity levels caused by inequivalent sites in 4*H*, 6*H*, and 15*R* SiC has been verified from a study of configuration coordinate phonons. From analyses of donor-acceptor pair and free-to-acceptor luminescence, two kinds of impurity levels of Al, Ga, and B acceptors and N donors substituted cubic-like and hexagonal-like sites are determined. All the impurities in cubic-like sites take deeper levels than those in hexagonal-like sites. Ratios of the ionization energies are approximately constant independent of polytypes and the kind of impurities, 1.0–1.08 for acceptors and 1.55–1.88 for donors, in spite of a wide range of the ionization energies. The origin of the site effect on the impurity level is explained by assuming the existence of a local dielectric constant and a local effective mass. Haynes' rule is found to apply relatively well to N donors in different sites in various polytypes SiC.

I. INTRODUCTION

SiC takes many crystal structures, namely polytypes, which are classified by the stacking sequence and cycle along the *c*-axis direction. Owing to long unit cells, many inequivalent sites exist for 4*H*, 6*H*, and 15*R* SiC in contrast to one kind for 3*C* SiC (zinc blende).[1] These inequivalent sites are divided into two kinds. One is a cubic-like arrangement of first- and second-neighbor atoms (*B* atom in the sequence of *ABC* in the close-packed structure) and the other is a hexagonal-like arrangement (*B* atom in the sequence of *ABA*).[1] Stacking sequences in the *c*-axis direction and numbers of cubic-like and hexagonal-like sites are given for 2*H*, 3*C*, 4*H*, 6*H*, and 15*R* SiC in Table I.

These inequivalent sites are expected to cause site-dependent impurity levels. The study of site-dependent impurity levels helps our understanding of the impurity level, because inequivalent sites play a role of perturbation on the impurity level. We have reported that site-dependent donor and acceptor levels exist in 6*H* SiC.[2] In the present report, the generality of the site-dependent impurity level is examined. Photoluminescence of 3*C*, 4*H*, 6*H*, and 15*R* SiC doped with Al, Ga, or B acceptors and N donors is studied, and general existence of the site-dependent donor and acceptor levels is verified. The donor and acceptor ionization energies in 4*H*, 6*H*, and 15*R* SiC are determined from analyses of the luminescence. Explanation of the origin of the site effect on the impurity level is tried based on the quantum-defect model. The site effect is well explained by assuming local physical constants around hexagonal-like and cubic-like sites. The result of this analysis predicts the existence of site-dependent impurity levels extensively in other polytype SiC crystals and, furthermore, in other materials. Although many materials such as ZnS and AgI indicate polytypism, there have been no reports on site-dependent impurity levels except for SiC, and no reports on the origin of this effect.

SiC crystals doped with Al acceptors and N donors emit bright visible luminescence due to donor-acceptor (D-A) pair transitions. The spectra of the luminescence in 4*H* and 6*H* SiC were reported to be composed of two kinds of series peaks.[3-5] Two different explanations have been given for these two series, and the donor levels determined in their reports differ as much as 100 meV from each other. Gorban *et al.*[3] and Suzuki *et al.*[4] explained that these two series in 4*H* and 6*H* SiC were zero-phonon lines and their LA phonon replicas. Hagen *et al.*[5] explained them to be due to two kinds of donor levels associated with cubic-like and hexagonal-like sites. In this report, confirmation that these two series are due to

TABLE I. SiC polytypes with two common notations and numbers of inequivalent sites.

Ramsdell notation	*ABC* notation	No. of inequivalent sites hexagonal-like	cubic-like
2*H* (wurzite)	*AB*	1	0
3*C* (zinc blende)	*ABC*	0	1
4*H*	*ABAC*	1	1
6*H*	*ABCACB*	1	2
15*R*	*ABCACBCABACABCB*	2	3

site-dependent donor levels is tried by studying configuration coordinate phonons of 3*C*, 4*H*, 6*H*, and 15*R* SiC, and good quantitative agreement is obtained.

II. EXPERIMENTAL PROCEDURE

A. Crystal growth

Crystals studied were epitaxial layers of 6*H* and 15*R* SiC (≃100–300 μm) and small single crystals of 3*C*, 4*H*, 6*H*, and 15*R* SiC (≃0.7× 0.7× 0.5 mm^3). The epitaxial layers were grown by the dipping technique using Si melts in graphite crucibles.[6] The small single crystals were nucleated on the walls of graphite crucibles[4,7] and holders during epitaxial growths.

Graphite of high purity (ash content less than 20 ppm, boron content less than 0.1 ppm) was used as a crucible material, and high-purity silicon was used. Acceptor materials were Al metal (99.999%), Ga metal (99.9999%), B powders (99.5%), and B_4C powders (99.9%). Donors were doped by using high-purity Ar gas (99.999%) mixed with 0.2 vol. % N_2 gas. The growth process was written about in our previous reports.[2,6]

The carrier concentration was measured by the Van der Pauw method at room temperature, and donor and acceptor concentrations were estimated using the temperature dependence of the carrier concentration in the literature.[8-11] This measurement was carried out only for epitaxial layers of 6*H* SiC, and the same value was assumed for 3*C*, 4*H*, and 15*R* SiC grown in the same growth run. Nominally undoped crystals were *n*-type of $n = 1.0 \times 10^{17}$ cm^{-3} (estimated donor concentration, $N_D \simeq 3\times 10^{17}$ cm^{-3}), which may be due to nitrogen contamination of the ambient from air. The crystal doped with 5×10^{-5} vol. % N_2 has had $n = 4.2 \times 10^{17}$ cm^{-3} ($N_N \simeq 1\times 10^{18}$ cm^{-3}). The crystals doped with 0.02–2.1 at. % Al metal had $p = 3.5 \times 10^{16}$–2.7×10^{18} cm^{-3} ($N_{Al} \simeq 1\times 10^{18}$–$1\times 10^{20}$ cm^{-3}). The amount of Ga metal was 0.5–2 at. %, and $p = 5.6\times 10^{15}$ cm^{-3} ($N_{Ga} \simeq 1\times 10^{18}$ cm^{-3}) for a 2 at. % Ga-doped sample. The amount of B was 0.02–0.5 at. %, and $p = 1.2\times 10^{15}$ cm^{-3} ($N_B \simeq 5\times 10^{18}$ cm^{-3}) for a 0.02 at. % B-doped sample.[12] The polytype was identified by using x-ray diffraction photographs and photoluminescence.

B. Optical measurements

Samples were excited by 365-nm light from a suitably filtered 250-W high-pressure Hg lamp or 325-nm light from a suitably filtered KEC He-Cd laser of about 10 mW. For weak excitation, weak light near the absorption edge from a Xe lamp monochromated by a Ritsu MC-20 monochromator was used. Spectra were measured using a Ritsu MC-30N monochromator and an HTV R636 photomultiplier. Raw spectra were normalized for the system response using an EOAL-101 standard lamp. Samples were immersed in liquid helium or nitrogen, or a cryostat with a heater was used. The temperature was monitored by a chromel-alumel thermocouple.

III. RESULTS AND DISCUSSION

A. General spectra

Figures 1(a)–1(c) show photoluminescence spectra of 4*H*, 6*H*, and 15*R* SiC doped with moderate amounts of Al, Ga, or B acceptors and N donors under low excitation at 4.2 K. Since the assignment of the spectra of 3C SiC has been established by extensive research,[13-18] results on 3C SiC are not shown here. The spectra are adjusted at zero-phonon peaks. These spectra are composed of two series of peaks, *B* and *C*, which are due to D-A pair transitions (Sec. III C). Another peak *A*, due to free-to-acceptor transitions (Sec. III B), appears at 77 K as shown in Figs. 2(a)–2(c) for 4*H*, 6*H*, and 15*R* SiC. Relative intensity of *A* peaks to *B* and *C* peaks varies from polytype to polytype and has a relation 15*R* > 3*C* ~ 4*H* > 6*H*. For the spectrum of 15*R* SiC at 77 K almost all the peaks are *A* peaks. The values of the ionization energies of donors have a relation 6*H* > 4*H* ≳ 15*R* > 3*C*, and those of acceptors are almost equal, independent of polytypes, as in Sec. IV. Therefore, this difference of the relative intensity may be due to the difference of the oscillator strength of the transitions between the conduction band and acceptor levels because of the difference of the conduction-band structure in various polytypes. Each of the D-A pair and free-to-acceptor peaks is composed of many smaller peaks, which seems to be caused by the same origin, because the separation energies are almost the same. The numbers of these peaks are one for 3C and 4*H*, two for 6*H*, and three or four for 15*R* SiC. The number of peaks increases with the increase of the number of inequivalent sites (see Table I).

Figures 1 and 2 show that the phonon replicas in the spectra of the samples doped with different acceptors are similar. Tentative phonons are indicated in the figures. Both D-A pair and free-to-acceptor peaks can be explained by assuming phonons common to all polytypes. The energies of phonons are $E_{TA} \simeq 28$, $E_{LA} \simeq 68$, $E_{TO} \simeq 95$, and two kinds of LO phonons of $E_{LO} \simeq 107$ and ≃118 meV. These values are in good agreement with the values determined by lattice absorption of 6*H* and 15*R* SiC,[19] and by Raman scattering of 3*C*, 4*H*, 6*H*, 15*R*, and 21*R* SiC.[20] Phonons of

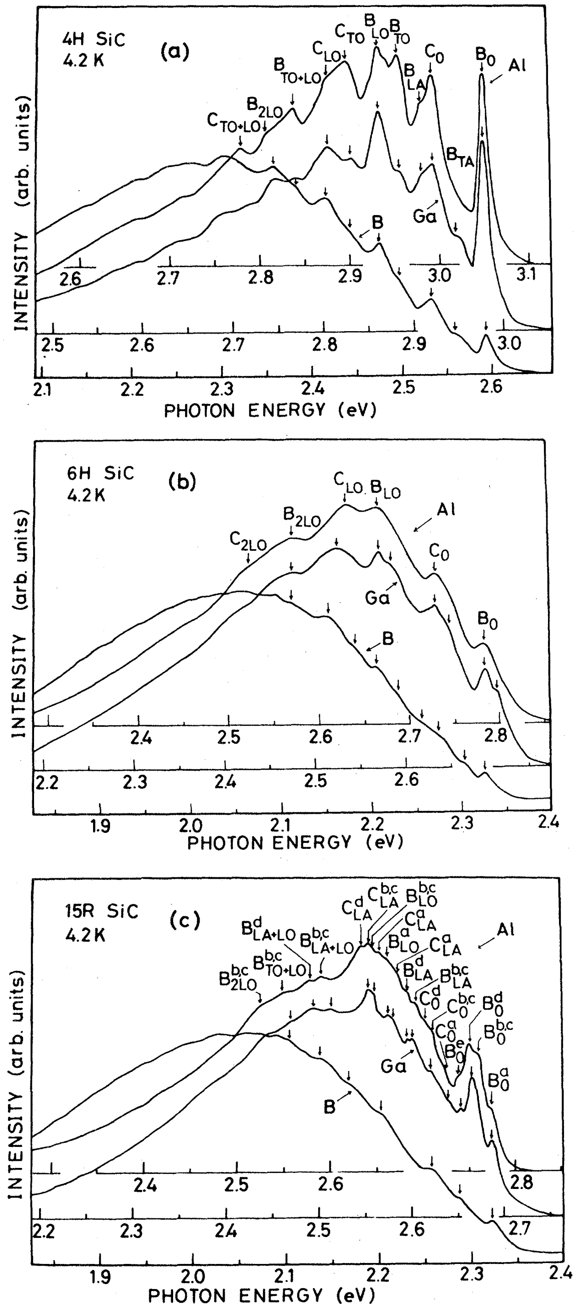

FIG. 1. Photoluminescence spectra of Al-doped, Ga-doped, and B-doped crystals of (a) 4*H*, (b) 6*H*, and (c) 15*R* SiC at 4.2 K. Subscripts indicate the kinds of phonons and superscripts indicate the kinds of sites which acceptors replaced.

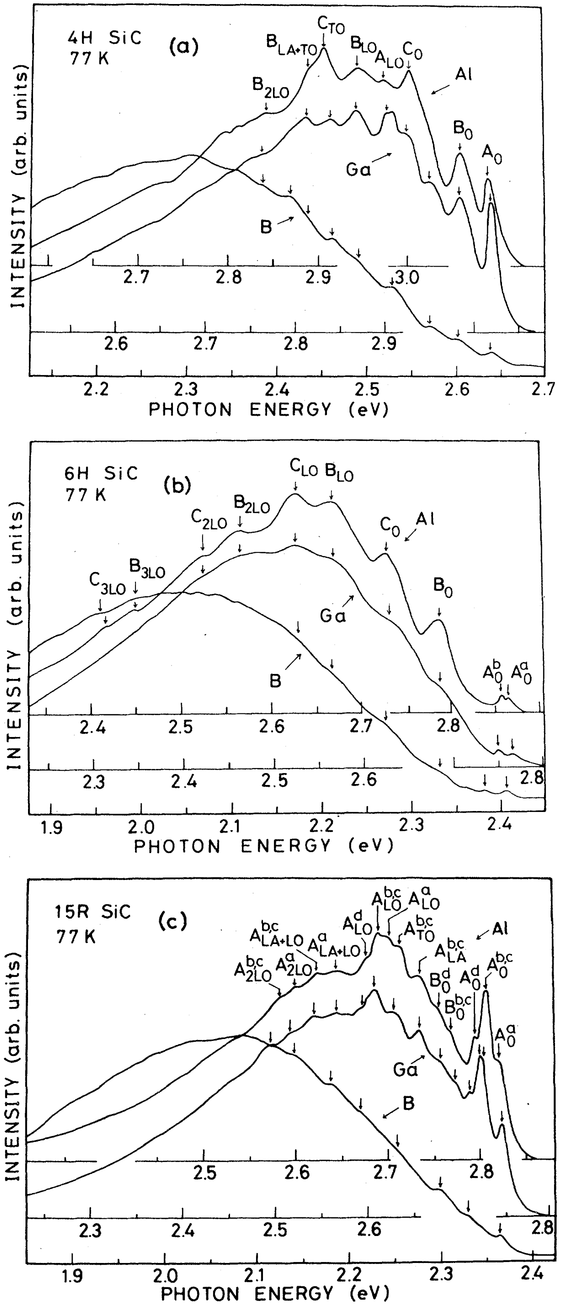

FIG. 2. Photoluminescence spectra of Al-doped, Ga-doped, and B-doped crystals of (a) 4*H*, (b) 6*H*, and (c) 15*R* SiC at 77 K. Subscripts indicate the kinds of phonons and superscripts indicate the kinds of sites which acceptors replaced.

nearly the same energy exist for various polytypes[20] because the Brillouin zones of these polytypes can be expressed by one standard large zone, which corresponds to that of wurzite (2*H*), by extending each normal Brillouin zone up to the large zone in the *c*-axis direction. The values of all the phonons observed here agree with those of phonons at Γ point reported by Feldman *et al.*[20] Two values of LO (Γ) phonon energies of $\simeq$120 and $\simeq$104 meV exist at the zone center and near the zone edge of the extended standard large zone, respectively.[20] For 3*C* SiC phonons of energies of $E_{\rm LO}(X) = 106$ and $E_{\rm LO}(\Gamma) = 120$ meV were assigned for the phonon replicas in the luminescence by Long *et al.*[13] However, the location of the conduction-band minimum varies from polytype to polytype,[21-24] and $E_{\mathrm{LO}} \simeq 107$ meV is commonly observed for 3*C*, 4*H*, 6*H*, and 15*R* SiC. Therefore, the 107-meV phonon seems to be more reasonably assigned to be an LO phonon at Γ point. For 4*H* SiC, TA phonon lines are observed in both Ga-doped and B-doped samples, but it is very weak in Al-doped samples as in Fig. 1(a). Similar results were reported for 3*C* SiC.[13-15]

B. Free-to-acceptor spectra

A peaks emerged at temperatures slightly below 77 K on the higher-energy side of B_0 peaks. *A* peaks broadened and became dominant over B_0 peaks with increasing temperature and indicated no shifts with the change of the excitation intensity. These characteristics are similar to that of free-to-acceptor transitions reported for 3*C* (Refs. 15–18) and 6*H* SiC.[2]

Free-to-acceptor transitions are expressed by a function of electron kinetic energy[25] as

$$I(E_K) = N_A^0 n(E_K)\sigma(E_K)v_{\mathrm{th}} . \tag{1}$$

Here, N_A^0 is the concentration of neutral acceptors, $n(E_K)$ the concentration of free electrons of kinetic energy E_K, and v_{th} the thermal velocity of the electrons. $\sigma(E_K)$ is the cross section for the radiative capture of a free electron by a neutral acceptor and is given as $\sigma(E_K) \simeq C_1 E_K^{-1/2}$.[2] The cross section is assumed to be the same for all the sites, because the properties of acceptors in different sites are approximately the same (Sec. IV). By expressing $n(E_K)$ and v_{th} as functions of E_K, Eq. (1) is transformed into the following relation:

$$I(E_K) = C E_K^{1/2} \exp(-E_K/kT) . \tag{2}$$

From Eq. (2) peak energy E_p is given by

$$E_p = E_{\mathrm{GX}} + E_{\mathrm{X}} - E_{\mathrm{A}} + \tfrac{1}{2}kT , \tag{3}$$

where E_{GX} is the exciton band gap and E_{X} is the free-exciton binding energy. Because of the existence of inequivalent sites given in Table I, many acceptor levels (E_{A}^i) are expected. In this case, Eq. (1) is transformed into

$$I(E_K) = C \sum_i E_{Ki}^{1/2} \exp(-E_{Ki}/kT) , \tag{4}$$

where $E_{Ki} = h\nu - E_{\mathrm{GX}} - E_{\mathrm{X}} + E_{\mathrm{A}}^i$ and $h\nu$ is the energy of emitted light.

The temperature dependences of $E_{\mathrm{GX}} - E_p$ for A_0 peaks of Ga-doped and B-doped 4*H* SiC and Ga-doped 15*R* SiC are shown in Figs. 3(a)–3(c). The values of E_{GX} were taken from reports,[23,26] and these values were confirmed by free-exciton luminescence measurements at 77 K.[27] $E_{\mathrm{GX}} - E_p$ indicates $\frac{1}{2}k$ dependence, within experimental uncertainty, for all the polytypes 3*C*,[15] 4*H*, 6*H*,[2] and 15*R* SiC doped with Al or Ga acceptors. As for B acceptors, 4*H* SiC indicated nearly $\frac{1}{2}k$ dependence [Fig. 3(b)]. In the case of B-doped 6*H* and 15*R* SiC crystals, $E_{\mathrm{GX}} - E_p$ did not indicate clear linearity with the temperature, which might be due to their broad peaks and due to interference by the defect luminescence[28] on the higher-energy side of A_0 peaks. When we dared to estimate slopes from linear parts of the lines, the slopes for B-doped 6*H* and 15*R* SiC crystals were about $\frac{1}{2}k$ or less. Kuwabara *et al.*[18] reported a slope of $0.7k$ for B-doped 3*C* SiC. Although the slope can be varied by the kinetic energy dependence of $\sigma(E_K)$, we take $\frac{1}{2}k$ dependence for B-doped 4*H*, 6*H*, and 15*R* SiC considering the experimental results. We can determine site-dependent acceptor levels from the extrapolations of $E_{\mathrm{GX}} - E_p$ lines to $T = 0$ as indicated in Fig. 3.

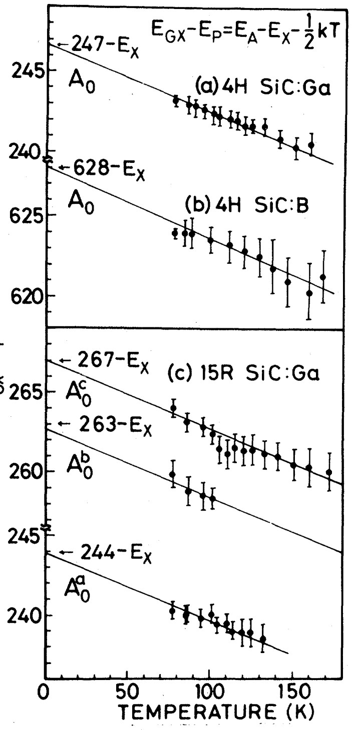

FIG. 3. Temperature dependences of $E_{\mathrm{GX}} - E_p = E_{\mathrm{A}} - E_{\mathrm{X}} - \frac{1}{2}\mathrm{kT}$ for *A* peaks of (a) Ga-doped 4*H* SiC, (b) B-doped 4*H* SiC, and (c) Ga-doped 15*R* SiC. The vertical bars indicate possible energy ranges of broad peaks.

Figures 4(a) and 4(b) show comparison of observed spectra and theoretical curves given by Eq. (4) (not shown for Ga-doped crystals). Good agreements are obtained for 3*C*,[15,17] 4*H*, and 6*H* SiC (Ref. 2) doped with Al or Ga acceptors. For 4*H* SiC two site-dependent acceptor levels exist, but only one impurity level is assumed in the cal-

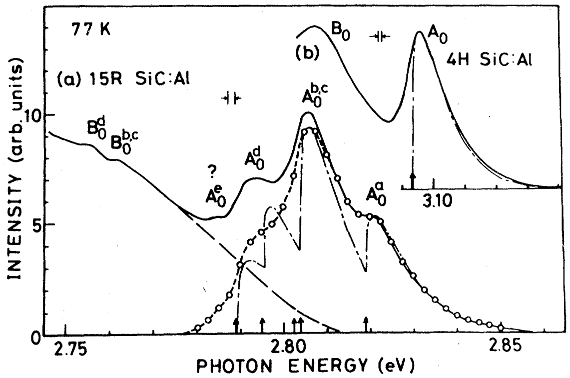

FIG. 4. Comparison of experimental spectra and calculated spectra at 77 K for (a) Al-doped 15*R* SiC and (b) Al-doped 4*H* SiC. The line with open circles of 15*R* SiC indicates spectrum of A_0 peaks after subtracting the background D-A pair spectrum assumed as the dashed line. The dot-dash lines indicate calculated spectra using Eq. (4) with $E_{GX}+E_X-E_A$ indicated by arrows.

culation. From the good agreement in Fig. 4(b), two inequivalent acceptor levels in 4*H* SiC are considered to be close to each other, probably within ±1 meV of experimental uncertainty. As to 15*R* SiC, spectra are complicated. A_0^a, $A_0^{b,c}$, and A_0^d peaks in Fig. 4(a) seem to be due to free-to-acceptor transitions. Based on the positions of $B_0^{b,c}$ and B_0^d peaks, the A_0^e peak seems to be overlapped with the B_0^a peak. (The A_0^e peak can be also considered as a TA phonon replica of $A_0^{b,c}$ peaks. However, the intensity of a TA phonon replica is generally very weak compared with that of the zero-phonon line, and the separation energy of 21 meV in the spectrum differs from the value determined in Sec. III A, $E_{TA}\simeq 28$ meV. Therefore, this does not seem to be the case.) Since it is difficult and uncertain to estimate the buried B_0^a peak properly, the background D-A pair spectrum is assumed as a simple line in the figure. For the curves after subtracting the background D-A pair spectra from the observed spectra, best fits are obtained for both Al-doped and Ga-doped 15*R* SiC crystals. Five inequivalent acceptor levels are assigned so that the best fits are obtained for both free-to-acceptor and D-A pair spectra (Sec. III D). The values of the three more shallow acceptor levels can be assigned with relatively high accuracy ($\simeq\pm 2$ meV), but the accuracy of the values of the two deeper acceptor levels seems to be rather bad, probably ±7 meV. The agreement of the acceptor levels determined from the temperature dependence of $E_{GX}-E_p$ and those by curve fitting is within ±1 meV for 3*C*, 4*H*, and 6*H* SiC,[2] but those of 15*R* SiC differ by about ±2 meV. For B-doped 4*H*, 6*H*, and 15*R* SiC crystals, curve fitting was not tried, because free-to-acceptor luminescence and defect luminescence[28] were overlapped, and background defect spectrum could not be properly determined. For B-doped 15*R* SiC, only two of five peaks are distinguished [Fig. 2(c)].

The free-exciton binding energies were reported to be 13.5 (Ref. 29) and 14 meV (Ref. 30) for 3*C* SiC, 20 meV for 4*H* SiC,[31] and 78 meV for 6*H* SiC.[32] The free-exciton binding energy of 15*R* SiC is estimated to be 40 meV from thermal quenching of free-exciton luminescence.[27] The acceptor ionization energies determined using E_A-E_X from curve fitting and the free-exciton binding energies E_X, are given in Table II. Considering the results of acceptors in 6*H* SiC (Ref.

TABLE II. Ionization energies of donors and acceptors in cubic-like sites (E^C) and hexagonal-like sites (E^H), their average ratios, and free-exciton binding energies (E_X) in 3*C*, 4*H*, 6*H*, and 15*R* SiC.

		Ionization energy (meV)				
	Site	N	Al	Ga	B	E_X
3*C*[a]	*C*	56.5	254	343	735	13.5[b]
6*H*	*C*	155	249	333	723	78[c]
	H	100	239	317	698	
	E^C/E^H	1.55	1.040	1.050	1.036	
15*R*	*C*	112	236	320	700	40
			230	311		
			223	305		
	H	64	221	300	666	
			206	282		
	E^C/E^H	1.75	1.076	1.072		
4*H*	*C*	124				20[d]
			191	267	647	
	H	66				
	E^C/E^H	1.88	1.0	1.0	1.0	

[a] References 14, 15, and 18.

[b] References 29 and 30.

[c] Reference 32.

[d] Reference 31.

2) and donors in 4*H*, 6*H*, and 15*R* SiC (Sec. III D), the three deeper levels are considered to belong to cubic-like sites for 15*R* SiC. The ionization energies of B acceptors are determined from the peak energies at 77 K using Eq. (3). The determined ionization energies of Al acceptors are in good agreement with those determined by Hall measurements of lightly doped samples, 230–250 meV for 6*H* SiC,[5] and about 240 meV for 4*H*, 6*H*, and 15*R* SiC.[9]

C. D-A pair spectra

At 4.2 K, *A*-series peaks disappeared and only *B*- and *C*-series peaks were observed. *B*- and *C*-series peaks shifted to the higher-energy side and broadened with increasing excitation intensity, and became broad and shifted to the higher-energy side with increasing donor and acceptor concentrations. Line spectra due to close pairs were observed[33] on the higher-energy side than the broad spectra due to distant pairs, in all the crystals of 3*C*, 4*H*, 6*H*, and 15*R* polytypes doped with small amounts of donors and acceptors. Peak shifts in time-resolved spectra were reported for Al-doped 4*H* and 6*H* SiC,[5] Al-doped and Ga-doped 4*H* SiC,[4] and Al-doped[13] and B-doped[15] 3*C* SiC. All these characteristics indicate that *B*- and *C*-series are due to D-A pair transitions.

In addition to these ordinary characteristics of D-A pair transitions, the peak intensity ratio of *B* and *C* peaks indicate strong dependence on excitation intensity and concentration of acceptors. Figure 5 shows that *B*-series peaks of Al-doped slightly *p*-type 4*H* SiC decrease more rapidly than *C*-series peaks with decreasing excitation intensity at 4.2 K. Pairs of peaks resolved in this figure (e.g., C_0 and B_1, B_2 and B_3) have probably been considered to be single peaks in the reports by Suzuki *et al.*[4] and Hagen *et al*,[5] and therefore their assignment of the peaks is different from the present one. At 77 K, *A*- and *B*-series peaks quench more rapidly than *C*-series peaks and finally disappear with decreasing excitation intensity for 4*H* [Fig. 6(a)], 6*H*,[2] and 15*R* SiC [Fig. 6(b)]. With increasing Al concentration, *B*-series peaks become weaker compared with *C*-series and finally disappear. Figures 7(a) and 7(b) compare spectra of slightly Al-doped samples under strong excitation and highly Al-doped samples under weak excitation for 4*H*, and 15*R* SiC at 4.2 K (for 6*H* SiC, see Ref. 2). These above-mentioned dependences on excitation intensity and doping were not observed for 3*C* SiC crystals grown in the same growth run as 4*H*, 6*H*, and 15*R* SiC crystals. Therefore, these characteristics seem to relate to the inequivalent sites which do not exist in 3*C* SiC. The peak intensity ratios of C_0 peaks to B_0 peaks under high excitation, where both *B*- and *C*-series appear with full

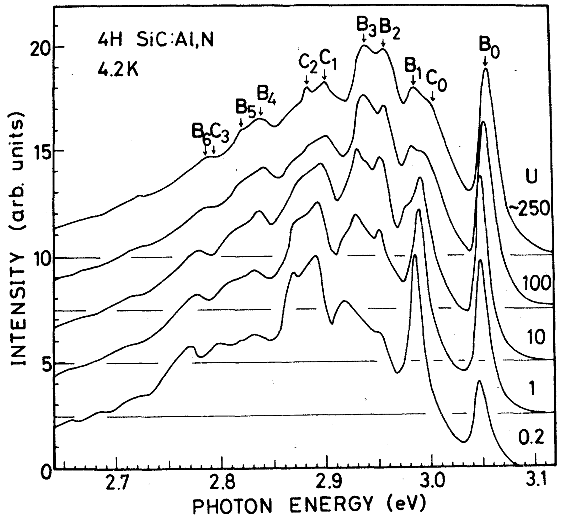

FIG. 5. Photoluminescence spectra of Al-doped slightly *p*-type 4*H* SiC ($N_N \simeq 3 \times 10^{17}$ cm^{-3}, $N_{Al} \simeq 1.5 \times 10^{18}$ cm^{-3}) at various excitation intensities (*U*) at 4.2 K.

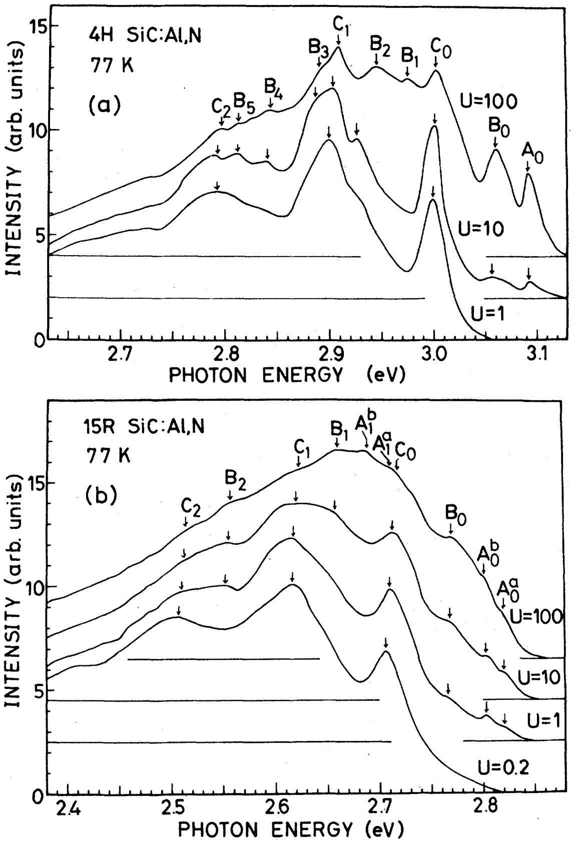

FIG. 6. Photoluminescence spectra of Al-doped (a) 4*H* SiC and (b) 15*R* SiC ($N_N \simeq 3 \times 10^{17}$ cm^{-3}, $N_{Al} \simeq 1.5 \times 10^{18}$ cm^{-3}) at various excitation intensities (*U*) at 77 K.

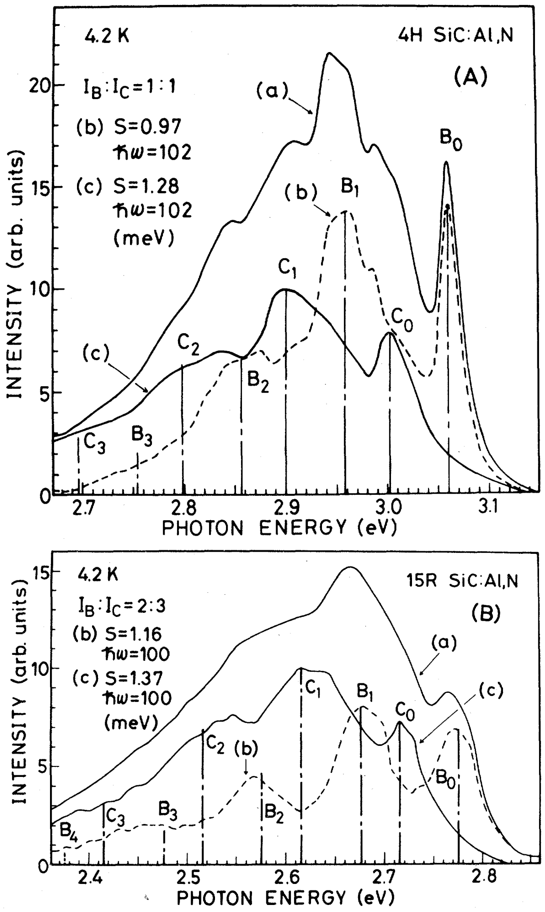

FIG. 7. Comparison of experimental D-A pair spectra and theoretical phonon spectra for Al-doped (A) 4*H* SiC, and (B) 15*R* SiC at 4.2 K. The vertical dot-dash lines indicate intensities of the phonon spectra calculated using Eq. (6) with parameters *S* and phonon energies $\hbar\omega$ indicated in the figures. (a) Spectra of slightly Al- and N-doped crystals under strong excitation with *B*- and *C*-series. (b) Spectra with only *B*-series, which are obtained by subtracting spectra (c) from spectra (a). The ratios of the total luminescence intensities of the spectra (b) to those of the spectra (c) are the same as the numbers of hexagonal-like sites to those of cubic-like sites. (c) Spectra of highly Al-doped crystals under weak excitation with only *C*-series.

intensities, are 0.96 for 4*H*, 1.9 for 6*H*, and 1.4 for 15*R* SiC, respectively. These values are in good agreement with the ratios of the numbers of cubic-like to hexagonal-like sites, i.e., 1 for 4*H*, 2 for 6*H*, and 1.5 for 15*R* SiC. Therefore, *B*- and *C*-series are assumed to be due to D-A pair transitions between acceptors and donors in hexagonal-like and cubic-like sites, respectively, as Hagen *et al.*[5] have suggested.

In order to verify this assumption, configuration coordinate phonon spectra are studied. We consider peaks of site-dependent acceptor levels as a single peak for simplicity. In the adiabatic approximation, the normalized line-shape function for multimode phonons is given by[34]

$$I_{ab}(E)=\sum_{m,n}\left(\sum_{n}\exp(-E_{bn}/kT)\right)^{-1}\exp(-E_{bn}/kT)$$
$$\times\,|\langle bn|M_{ba}|am\rangle|^{2}\delta(E_{bn}-E_{am}-E)\,. \qquad (5)$$

Here, M_{ba} is the dipole matrix element between the electronic ground and excited states, *a* and *b*. The adiabatic potentials E_{am} and E_{bn} are for the vibrational wave functions in the ground state $|am\rangle$ and the excited state $|bn\rangle$, respectively. Integers *m* and *n* are indices for the ground and excited vibrational states, respectively. Based upon this equation, there are no terms which represent the number of luminescent centers and the photon number. Physically the interaction between the lattice vibration and the luminescent center, which determines phonon spectrum, may not be affected by the numbers of photons and luminescent centers. Therefore, if *C*-series are LA phonon replicas of *B*-series as Gorban *et al.*[3] and Suzuki *et al.*[4] have suggested, strong dependences on excitation intensity and acceptor concentration are not expected. Since the D-A pair spectra exhibit strong dependences on excitation intensity and acceptor concentration, the *C*-series are not LA phonon replicas of the B_0 peak.

The line-shape function for a single mode at $T\simeq 0$ on the Condon and the linear-mode approximations is obtained from Eq. (5) as[35]

$$I_{ab}(E)=\sum_{m=0}^{\infty}\exp(-S)\,\frac{S^{m}}{m!}\,\delta(m\hbar\omega_{P}-E_{ab}+S\hbar\omega_{P}-E)\,, \qquad (6)$$

where the value *S* represents the degree of localization of electrons and holes to impurity atoms and $\hbar\omega_P$ is the energy of a phonon. This leads to an emission spectrum consisting of a series of evenly spaced lines at

$$E_{m}=(E_{ab}-S\hbar\omega_{P})-m\hbar\omega_{P}=E_{0}-m\hbar\omega_{P}\,. \qquad (7)$$

In Figs. 7(a) and 7(b), the spectrum of a strong *p*-type crystal under low excitation condition is taken for the *C*-series spectrum [curve (*c*)]. The *B*-series spectrum [curve (b)] is obtained by subtracting the *C*-series spectrum from the combined *B*- and *C*-series spectrum [curve (a)] in such a way that the ratio of the total luminescence intensity of the *B*-series spectrum to that of the *C*-series spectrum is equal to the ratio of the numbers of cubic-like sites to hexagonal-like sites. Both *B*- and *C*-series spectra of 4*H*, 6*H*,[2] and 15*R* SiC are fairly well described by Eq. (6) using appropriate values of *S* and $\hbar\omega_P$. The rather poor agreement for the case of 15*R* SiC is due to the lack of a properly Al-doped p-type sample.[36] Peak intensity ratios of C_0 to B_0 peaks, values of S, sums of donor and acceptor ionization energies averaged among sites, and $\hbar\omega_P$ are given in Table III. The donor ionization energy E_D will be determined in Sec. III D. The S parameter increases with increasing $E_D + E_A$, except for 3C SiC. This is consistent with the meaning of the S parameter which implies the strength of the binding energy or degree of localization of electrons and holes to luminescent centers. Increase of S with increase of $E_D + E_A$ was also reported for GaP.[37] The observed phonons with energies of 100–106 meV correspond to the smaller LO phonon described in Sec. III A. The small value of the S parameter in the case of 3C SiC may be due to the large phonon energy.[38]

The fair agreement of the resultant spectra with Eq. (6) supports the idea that B- and C-series peaks are due to donors in inequivalent sites with different binding energies. Dependences of the intensity ratio of B- and C-series on excitation intensity and acceptor concentration are also observed in Ga-doped and B-doped samples. But in these cases, quenching of the B-series peak is not so remarkable, probably due to small concentrations of Ga and B acceptors owing to their small solubility limits in SiC.[10]

The dependences of the intensity ratio of B- and C-series peaks on excitation intensity and acceptor concentration can be explained by the ratio of the occupied donors in cubic-like sites to those in hexagonal-like sites. The occupation probability is expressed by the Fermi level and the electron quasi-Fermi level.

(1) When a sample is strong p-type, the Fermi level is near the acceptor level. In this case, the ratio of the numbers of occupied donors in different sites is

$$N^H/N^C \simeq \tfrac{1}{2}\exp[-(E^C - E^H)/kT] \ll 1 \qquad (8)$$

using Boltzmann distribution. Here, N^H and N^C are the numbers of donors in hexagonal-like sites and in cubic-like sites, respectively. Therefore, transitions due to donors in hexagonal-like sites are far fewer than those in cubic-like sites, and only C-series are observed.

(2) When concentrations of donors and acceptors are small, the electron quasi-Fermi level may be higher than both donor levels, because the number of donors is smaller than the number of generated electrons. Therefore, B- and C-series peaks are comparable at low temperatures. However, when the temperature is raised, a larger portion of electrons at shallower donors in hexagonal-like sites are thermally excited compared with those at deeper donors in cubic-like sites. Therefore, with decreasing excitation intensity, the electron quasi-Fermi level descends and the number of occupied donors in hexagonal-like sites decreases more rapidly than that in cubic-like sites and B-series disappear.

D. Donor levels

Donor levels are estimated from D-A pair spectra using the acceptor levels determined in Sec. III B. The energy relation for D-A pair transitions is written

$$h\nu_{\text{D-A}} = E_G - (E_A + E_D) + e^2/4\pi\epsilon R \,. \qquad (9)$$

For the case of weak excitation and for $N_A \gg N_D$, $a_A^3 N_A \ll 1$ and $a_D^3 N_D \ll 1$, the dependence of luminescence intensity on the pair distance (R) can be approximated by[39]

$$I(R) \propto R^6 \exp(-\tfrac{4}{3}\pi N_A R^3) \,, \qquad (10)$$

where a_A and a_D are the Bohr radii of a hole and an electron, respectively. The estimated Al concentration of an Al-doped sample is $N_{\text{Al}} \simeq 1\times10^{18}$ cm^{-3} ($p = 3.5\times10^{16}$ cm^{-3}), the Ga concentration of a Ga-doped sample $N_{\text{Ga}} \simeq 1\times10^{18}$ cm^{-3} ($p = 5.6\times10^{15}$ cm^{-3}), and the N concentration of all samples $N_N \simeq 3\times10^{17}$ cm^{-3} ($n = 1.0\times10^{17}$ cm^{-3}). The 3C, 4H, and 15R SiC samples were grown in the same growth run. The Bohr radius is modified

TABLE III. Numbers of cubic-like and hexagonal-like sites, ratios of C_0 to B_0 peak intensities, S parameters, sums of the donor and acceptor ionization energies averaged among sites, and phonon energies for 3C, 4H, 6H, and 15R SiC.

	Site	No. of sites	$I(C_0)/I(B_0)$	S	$E_D + E_A$ (meV)	$\hbar\omega_P$ (meV)
3C	C	1	1/0	1.06	311[a]	116
	H	0				
6H	C	2	1.9/1	1.70	404	106
	H	1		1.32	339	104
15R	C	3	2.8/2	1.37	342	100
	H	2		1.16	278	100
4H	C	1	0.96/1	1.28	315	102
	H	1		0.97	257	102

[a] Reference 15.

with the observed activation energy in the quantum-defect model (Sec. IV). The modified Bohr radii [$a^*\nu$ in Eqs. (12) and (13) in Sec. IV] of N in hexagonal-like sites are $\simeq$8–15 Å, those of N in cubic-like sites are $\simeq$6–10 Å, those of Al in both kinds of sites are $\simeq$4 Å, and those of Ga in both kinds of sites are $\simeq$3.5 Å in all polytypes.[40] These values satisfy the conditions that $N_A \gg N_D$, $a_A^3 N_A \ll 1$, and $a_D^3 N_D \ll 1$. The B_0 peak due to transitions between donors in shallower hexagonal-like sites and acceptors in inequivalent sites, is used to determine the ionization energy of N donors. On the assumption that the capture cross section, the pair distribution function, and the pair occupation probability do not depend on the inequivalent site which an impurity atom substitutes, the shape function of the D-A pair spectrum is written as

$$I(E) \propto \sum_i E_i^{-6} \exp[-\tfrac{4}{3}\pi N_A (e^2/4\pi\epsilon E_i)^3] , \qquad (11)$$

where $E_i = E - E_G + E_D + E_A^i$ is the Coulomb energy between the donor in the hexagonal-like site and an acceptor in one of the inequivalent sites, and E_A^i is the ionization energy of the acceptor at the ith inequivalent site.

The Coulomb energy is estimated by curve fitting between calculated spectrum using Eq. (11) and experimental spectrum under low excitation at 4.2 K. Figures 8(a) and 8(b) show best fits between theoretical and experimental spectra. The energies of $E_G - E_D - E_A^i$ are indicated by arrows in Figs. 8(a) and 8(b). The donor ionization energy is determined with the value of $E_G - E_D - E_A^i$ and the acceptor ionization energy determined in Sec. III B. For Al-doped 3C SiC, $E_G - E_D - E_A = 2.0925$ eV, $N_A = 1.5 \times 10^{18}$ cm^{-3}, and $E_N = 57$ meV are obtained. For 4H SiC, $E_G - E_D - E_A = 3.0485$ eV, $N_A = 1.5 \times 10^{18}$ cm^{-3}, and $E_N^H = 66$ meV are obtained for the Al-doped sample, and $E_G - E_D - E_A = 2.9515$ eV, $N_A = 1.5 \times 10^{18}$ cm^{-3}, and $E_N^H = 66$ meV for the Ga-doped sample. For 15R SiC, $E_G - E_D - E_A^a = 2.7605$ eV, $N_A = 1.5 \times 10^{18}$ cm^{-3}, and $E_N^H = 63$ meV are obtained for the Al-doped sample, and $E_G - E_D - E_A^a = 2.6785$ eV, $N_A = 1.5 \times 10^{18}$ cm^{-3}, and $E_N^H = 64$ meV for the Ga-doped sample. The acceptor concentrations determined from curve fitting and those estimated from Hall measurements are in good agreement. Since defect spectra[28] overlapped D-A pair spectra and the D-A pair spectra were broad, fitting was not tried for B-doped samples. From the separation energy of B_0 and C_0 peaks of 58 meV, $E_N^C = 124$ meV is determined for N donors in cubic-like sites for 4H SiC. Similarly, from the separation energy of 48 meV, $E_N^C = 112$ meV is determined for N donors in cubic-like sites for 15R SiC. The ionization energy of N of 56.5 meV in 3C SiC was determined using D-A pair line spectrum by Kuwabara *et al.*[15] Our value of 57 meV is in good agreement with their value. Therefore, the accuracy of the determined donor levels seems to be rather high, probably ±3 meV. The agreement of the donor levels determined from Al-doped and Ga-doped SiC crystals is very good, ±1 meV. These donor levels are given in Table II. For 6H SiC, values in our previous report[2] are used. The ionization energies of N donors determined by Hall measurements, 49 (Ref. 42) and 50 meV (Ref. 43) for 3C SiC, 33 meV (Ref. 9) for 4H SiC, 95 meV (Refs. 8, 9) for 6H SiC, and 52 (Ref. 8) and 47 meV (Ref. 9) for 15R SiC are slightly smaller than the present values of hexagonal-like sites, which might be caused by the screening by ionized impurities and the assumption of a single donor level in their analyses.

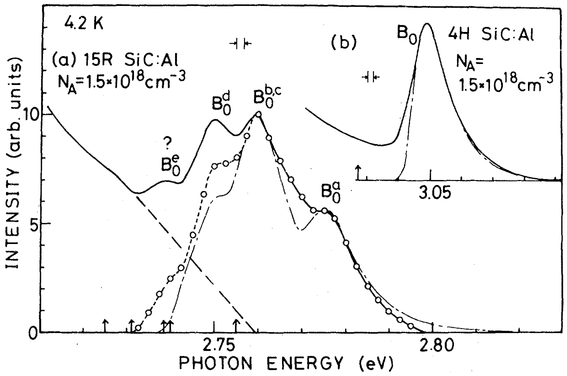

FIG. 8. Comparison of experimental spectra at 4.2 K and calculated spectra for (a) Al-doped 15R SiC and (b) Al-doped 4H SiC. The line with open circles of 15R SiC indicates spectrum of B_0 peaks after subtracting the background B_1 peak assumed as the dashed line. The dot-dash lines indicate calculated spectra using Eq. (11) with written acceptor concentrations and $E_{GX} - E_D - E_A^i$ indicated by the arrows.

IV. ORIGIN OF THE SITE EFFECT

Table II shows the donor ionization energies, the acceptor ionization energies, the average ratios of the ionization energies of donors and acceptors in cubic-like sites to those in hexagonal-like sites, and the free-exciton binding energies from literatures.[29-32] From these values, the following characters of the donor and acceptor ionization energies are deduced.

(1) Donor levels markedly depend on sites and polytypes.

(2) Acceptor levels slightly depend on sites and polytypes, and the activation energy decreases with the increase of the hexagonality (percentage of the number of hexagonal-like sites in all the sites: 0 for 3C, $\frac{1}{3}$ for 6H, $\frac{2}{5}$ for 15R, $\frac{1}{2}$ for 4H).

(3) The activation energies of impurities in cubic-like sites (E^C) are larger than those in hexagonal-like sites (E^H). For donors the ratios of E^C/E^H are large and are 1.55–1.88, and for acceptors E^C/E^H are nearly one and are 1.0–1.08.

The commonly used theories on impurity levels, the effective mass theory, and the quantum-defect model require a unique impurity level for an impurity atom, since a specific effective mass and a dielectric constant exist for one material. The existence of site-dependent impurity levels seems to imply inapplicability of these theories to this case. However, the nearly constant ratios of E^C/E^H suggest the existence of certain localized physical constants around a cubic-like or a hexagonal-like site, and these theories are still available. This idea is assisted by the fact that the nearest-neighbor atomic configurations are the same for cubic-like or hexagonal-like sites independent of polytypes. By assuming such localized physical constants, explanation of the characteristics of the site-dependent impurity levels is tried on the basis of the quantum-defect model, because the effective-mass theory gives too small ionization energies of 0.2–0.5 times of the observed values.

In the quantum-defect model,[44] the effective principal quantum number ν is determined from the observed impurity ionization energy, $E(\text{obs})$, by

$$E(\text{obs}) = -m^* e^4/2\hbar^2\epsilon^2\nu^2 = -e^2/2\epsilon a^*\nu^2\,, \tag{12}$$

where

$$a^* = \hbar^2\epsilon/m^* e^2\,. \tag{13}$$

Here, a^* is referred to as the effective Bohr radius. We assume that ν is inherent in the kind of an impurity atom, since ν is the correction factor for the effect of core potential of the impurity atom. In this model, factors which depend on the inequivalent sites are the dielectric constant and the effective mass.

The modified Bohr radii $a^*\nu$ of donors are 6.1–13.9 Å and those of acceptors are 2.2–4.2 Å.[40] Although the hole modified Bohr radii are a little larger than the distance to the nearest-neighbor atoms, 3.08 Å in the a-axis direction and 2.54 Å in the c-axis direction,[45] we assume that electron and hole wave functions are localized around cubic-like and hexagonal-like sites for simplicity. In this case we may use the dielectric constants and effective masses of 3C and 2H SiC in place of those around cubic-like and hexagonal-like sites. The static dielectric constant of 3C SiC was reported as $\epsilon_S = 9.72$.[41] The static dielectric constants of 2H SiC were determined to be $\epsilon_S(\perp) = 9.57$ and $\epsilon_S(\|) = 10.73$ (Ref. 46) in the same way as in Ref. 41. The ratio of squares of the dielectric constants is

$$[2\epsilon_S(\perp, 2H)^2 + \epsilon_S(\|, 2H)^2]/3\epsilon_S(3C)^2 = 1.052\,. \tag{14}$$

For 3C SiC, the density-of-states electron effective mass has been determined by various methods,[42,43,47] but those values largely differ from each other. Moreover, there have been no reports on the electron effective mass for 2H SiC. Therefore, the electron effective masses estimated from the curvatures of the conduction-band minima are used.[48] For 3C SiC, $m_\perp^* = 0.24m_0$ and $m_\|^* = 1.12m_0$ are obtained, and for 2H SiC $m_\perp^* = 0.26m_0$ and $m_\|^* = 0.70m_0$. The ratio of the effective masses is obtained as

$$[2m_e^*(\perp, 3C)^2 + m_e^*(\|, 3C)^2]^{1/2}/[2m_e^*(\perp, 2H)^2 + m_e^*(\|, 2H)^2]^{1/2} = 1.48\,. \tag{15}$$

Since the valence-band maxima of SiC are located at the Γ valley and are nearly spherical independent of polytypes,[9,21,22] the hole effective masses of different polytypes may be nearly constant, whereas, the conduction-band minima of different polytypes are located at different valleys[9,21-24]: X valleys for 3C SiC and K valleys for 2H SiC. Therefore, the electron effective masses vary from polytype to polytype. Since the physical constant affecting the acceptor level is only the dielectric constant, the ratio of the acceptor activation energies is expected to be 1.052. This value is in good agreement with the observed values of 1.0–1.076. Since both the electron effective mass and the dielectric constant affect the donor activation energy as in Eq. (12), the ratio becomes 1.052 × 1.48 = 1.56. This value is in good agreement with the observed values of 1.55–1.88. These fairly good agreements support the existence of the localized effective mass and the dielectric constant. However, the variation of the ratio in different polytypes and sites needs more advanced treatment taking account of the atomic configuration farther than the nearest-neighbor atoms and needs more accurate values of the effective masses.

V. HAYNES' RULE

The exciton binding energies (E_{BX}) (Ref. 49) versus the ionization energies (E_{D}) of N donors of 3C, 4H, 6H, and 15R SiC are shown in Fig. 9. This figure shows that Haynes' rule[50] applies relatively well to SiC. Choyke *et al.*[51] suggested the inapplicability of this rule to SiC, which might be caused by uncertain ionization energies they had estimated. The energy ratio, namely the ratio of exciton binding energies to ionization energies ($E_{\mathrm{BX}}/E_{\mathrm{D}}$) for N donors is about 0.17. Theoretical calculations[52] indicate that the energy ratio is nearly constant of about 0.1 in the range

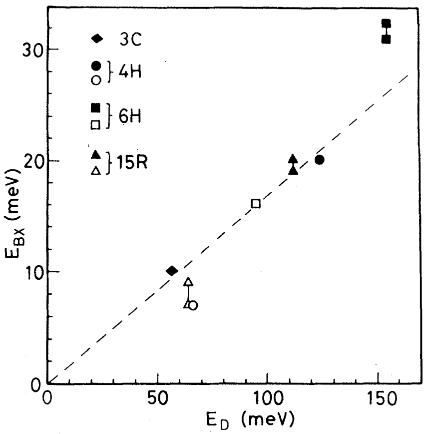

FIG. 9. Exciton binding energies (E_{BX}) versus ionization energies (E_D) for N donors in 3*C*, 4*H*, 6*H*, and 15*R* SiC. Open symbols indicate the data for donors in hexagonal-like sites and closed symbols for donors in cubic-like sites.

of the mass ratio (m_e^*/m_h^*) more than 0.2 which various SiC polytypes may have. Therefore, Haynes' rule can be applied even if the mass ratio varies among SiC polytypes and different sites. The data points of donors in hexagonal-like sites (open symbols in Fig. 9) tend to deviate from the line of 0.17 in the direction of smaller values of energy ratio, and those in cubic-like sites (closed symbols) in the direction of larger values of energy ratio. Since the mass ratio of cubic-like sites are larger than that of hexagonal-like sites (Sec. IV), the energy ratio should increase with the increase of the mass ratio. This relation is explained by the calculation by Sharma,[53] whereas the other researchers[52] have reported that the energy ratio decreases or does not change with increasing mass ratio.

VI. SUMMARY

The peculiar characteristics of D-A pair and free-to-acceptor luminescence in 4*H*, 6*H*, and 15*R* SiC have been explained, assuming site-dependent donor and acceptor levels. Good agreement was obtained between the number of sites and the intensity of the photoluminescence associated with a given site, which indicates that every impurity atom enters each kind of site in equal probability. The applicability of Haynes' rule to SiC was shown, and therefore the donor ionization energies can be roughly estimated from the exciton binding energies with a slight modification by the site-dependent effective masses. The origin of the site effect on the impurity level was explained by assuming a local dielectric constant and a local effective mass on the basis of the quantum-defect model. From these results, the site effect on the impurity levels is expected to exist extensively in other polytype SiC crystals, and furthermore, in other materials such as ZnS and AgI, provided that the local effective masses or the local dielectric constants differ considerably.

ACKNOWLEDGMENTS

The authors wish to thank Dr. H. Kuwabara for valuable discussion. They wish to express deep gratitude to Dr. W. F. Knippenberg, Dr. R. M. Potter, and Dr. I. Swiderski for their supply of SiC crystals grown by the Lely method. They are very grateful to Dr. L. A. Hemstreet for his estimation of the effective masses. The authors wish to thank the Nihon Silicon Co. for the supply of pure Si and the Taiheiyo Kogyo Co. and Syowa Denko Co. for the supply of industrial-grade SiC crystals.

---

*Present address: Takuma College of Electro-Communications, Takuma 769-11, Kagawa, Japan.

[1] L. Patrick, Phys. Rev. 127, 1878 (1962). Hexagonal sites in *the pure hexagonal structure* 2*H* belong to the space group of C_{6v} and cubic sites in *the pure cubic structure* 3*C* belong to T_d. However, hexagonal-like sites and cubic-like sites in other polytypes belong to the same space group of C_{3v}. Therefore, a labeling scheme of the sites based on group theory is not suitable, and conventional notations of "cubic-like" and "hexagonal-like" are employed in the present report.

[2] M. Ikeda, H. Matsunami, and T. Tanaka, J. Lumin. 20, 111 (1979).

[3] I. S. Gorban, V. A. Gubanov, and V. M. Efimov, Fiz. Tverd. Tela 14, 2324 (1973) [Sov. Phys.—Solid State 14, 2010 (1973)].

[4] A. Suzuki, H. Matsunami, and T. Tanaka, J. Phys. Chem. Solids 38, 693 (1977); J. Electrochem. Soc. 124, 241 (1977).

[5] S. H. Hagen, A. W. C. van Kemenade, and J. A. W. van der Does de Bye, J. Lumin. 8, 18 (1973).

[6] A. Suzuki, M. Ikeda, N. Nagao, H. Matsunami, and T. Tanaka, J. Appl. Phys. 47, 4546 (1976).

[7] Y. Inomata, Z. Inoue, M. Mitomo, and H. Tanaka, J. Ceram. Soc. Jpn. 77, 83 (1969).

[8] S. H. Hagen and C. J. Kapteyns, Philips Res. Rep. 25, 1 (1970).

[9] G. A. Lomakina, Yu. A. Vodakov, E. N. Mokhov, V. G. Oding, and G. F. Kholuyanov, Fiz. Tverd. Tela 12, 2918 (1970) [Sov. Phys.—Solid State 12, 2356 (1971)]; G. A. Lomakina, in *Silicon Carbide*—1973, edited by R. C. Marshall, J. W. Faust, Jr., and C. E. Ryan (University of South Carolina Press, Columbia, 1974), p. 520.

[10] Yu. A. Vodakov, G. A. Lomakina, E. N. Mokhov, E. I. Radovanova, V. I. Sokolov, M. M. Usmanova,

G. F. Yuldashev, and B. S. Machmudov, Phys. Status Solidi A 35, 37 (1976).

[11] G. A. Lomakina, Fiz. Tverd. Tela 7, 600 (1965) [Sov. Phys.—Solid State 7, 475 (1965)].

[12] This value of B concentration seems to be a little too large, which may be caused by the experimental uncertainty due to high resistivity of this sample. This value is about one order of magnitude higher than the reported one in W. E. Nelson, F. A. Halden, and A. Rosengreen, J. Appl. Phys. 37, 333 (1966).

[13] N. N. Long, D. S. Nedzvetskii, N. K. Prokofeva, and M. B. Reifman, Opt. Spectrosc. 30, 165 (1971).

[14] H. Kuwabara, K. Yamanaka, and S. Yamada, Phys. Status Solidi A 37, K157 (1976).

[15] H. Kuwabara, doctoral thesis, University of Osaka, 1978 (unpublished). His present address is Dept. of Electrics, College of Engineering, Sizuoka Univ., Hamamatsu 432, Japan.

[16] G. Zanmarchi, J. Phys. Chem. Solids 29, 1727 (1968).

[17] N. N. Long and D. S. Nedzvetskii, Opt. Spectrosc. 35, 645 (1973).

[18] H. Kuwabara and S. Yamada, Phys. Status Solidi A 30, 739 (1975).

[19] L. Patrick and W. J. Choyke, Phys. Rev. 123, 813 (1961).

[20] D. W. Feldman, J. H. Parker, Jr., W. J. Choyke, and L. Patrick, Phys. Rev. 173, 787 (1968).

[21] H. G. Junginger and W. van Haeringen, Phys. Status Solidi 37, 709 (1970).

[22] L. A. Hemstreet and C. Y. Fong, in *Silicon Carbide—1973*, edited by R. C. Marshall, J. W. Faust, Jr., and C. E. Ryan (University of South Carolina Press, Columbia, 1974), p. 284.

[23] L. Patrick, W. J. Choyke, and D. R. Hamilton, Phys. Rev. 137, A1515 (1965).

[24] L. Patrick, Phys. Rev. B 5, 2198 (1972).

[25] K. Colbow, Phys. Rev. 141, 742 (1966).

[26] L. Patrick, D. R. Hamilton, and W. J. Choyke, Phys. Rev. 132, 2023 (1963).

[27] M. Ikeda and H. Matsunami, Phys. Status Solidi A 58, 657 (1980).

[28] V. V. Makarov, Fiz. Tverd. Tela 9, 596 (1967) [Sov. Phys.—Solid State 9, 457 (1967)].

[29] D. S. Nedzvetskii, B. V. Novikov, N. K. Prokofeva, and M. B. Reifman, Fiz. Tekh. Poluprovodn. 2, 1089 (1968) [Sov. Phys.—Semicond. 2, 914 (1969)].

[30] V. A. Kiselev, B. V. Novikov, M. M. Pimonenko, and E. B. Shadrin, Fiz. Tverd. Tela 13, 1118 (1971) [Sov. Phys.—Solid State 13, 926 (1971)].

[31] G. B. Dubrovskii and V. I. Sankin, Fiz. Tverd. Tela 17, 2776 (1975) [Sov. Phys.—Solid State 17, 1847 (1975)].

[32] V. I. Sankin, Fiz. Tverd. Tela 17, 1820 (1975) [Sov. Phys.—Solid State 17, 1191 (1975)].

[33] Analysis of the line spectra could not be carried out, since separation of the different series due to donors and acceptors in inequivalent sites was impossible at the present state.

[34] R. C. O'Rourke, Phys. Rev. 91, 265 (1953).

[35] T. H. Keil, Phys. Rev. 140, A601 (1965).

[36] When the amount of Al metal in the Si growth melt was increased, the polytype of grown layers became different from 15R SiC of substrates and were always mixtures of 6H and 15R SiC. As a result, a pure 15R SiC crystal of strong p type could not be obtained. The spectrum without B-series in Fig. 7 (B) was obtained by measuring a sample with $p=3.3\times10^{17}$ cm^{-3} under very weak excitation. Compare the hole concentration with those of 4H and 6H SiC of 2.7×10^{18} cm^{-3} and 2.4×10^{18} cm^{-3}, respectively.

[37] M. Tajima and M. Aoki, Jpn. J. Appl. Phys. 13, 812 (1974).

[38] Although the condition is slightly different, in the case of an electron bound to an impurity, the S parameter is given as $S=E_i(\epsilon_S/n_0^2-1)/\hbar\omega_P$, where E_i is the binding energy of the impurity, ϵ_S the static dielectric constant, and n_0 the refractive index (Ref. 16), or $S \propto (\epsilon_\infty^{-1}-\epsilon_S^{-1})/\hbar\omega_P v_0^{1/3}$, where ϵ_∞ is the high-frequency dielectric constant and v_0 the volume of the unit cell; T. Toyozawa, in *Dynamic Processes in Solid State Optics*, edited by R. Kubo and H. Kamimura (Syokabo and Benjamin, Tokyo and New York, 1967), p. 110. These relations indicate that the S parameter decreases in inverse proportion to the increase of $\hbar\omega_P$.

[39] R. Bindemann and K. Unger, Phys. Status Solidi B 66, 133 (1974); L. V. Takunov, Fiz. Tekh. Poluprovodn. 10, 2190 (1976) [Sov. Phys.—Semicond. 10, 1302 (1976)].

[40] The modified Bohr radius defined as $a^*\nu$ was estimated with the following data. Density-of-states effective mass m_e^* was taken from the estimated values: $m_e^*(3C)=0.30m_0$, $m_e^*(4H)=0.37m_0$, $m_e^*(6H)=0.65m_0$, and $m_e^*(15R)=0.31m_0$, by Y. M. Tairov and Y. A. Vodakov, in *Electroluminescence*, edited by J. I. Pankov (Springer, New York, 1977), p. 31. The hole effective masses of all the polytypes were assumed to be $1.0m_0$: H. J. van Daal, W. F. Knippenberg, and J. D. Wasscher, J. Phys. Chem. Solids 24, 109 (1963). The static dielectric constants in Ref. 41 were used for 3C and 6H SiC. The static dielectric constants of 4H and 15R SiC were calculated by the method in Ref. 41 using the refractive index in P. T. B. Shaffer, Appl. Opt. 10, 1034 (1971), and phonon energies in Ref. 20. $\hbar\omega_L$ was assumed to be the same as that of 6H SiC, since $\hbar\omega_L$ was almost independent of polytypes [Ref. 20]. The calculated static dielectric constants were $\epsilon_S(\perp)=9.76$ and $\epsilon_S(\parallel)=10.32$ for 4H SiC, and $\epsilon_S(\perp)=9.72$ and $\epsilon_S(\parallel)=10.10$ for 15R SiC. The obtained modified Bohr radii $a^*\nu$ were for 3C SiC: 15.0 Å for N, 3.9 Å for Al, 3.3 Å for Ga, and 2.3 Å for B; for 4H SiC: 12.5 and 9.1 Å for N in hexagonal-like sites (HS) and cubic-like sites (CS), respectively, 4.5 Å for Al, 3.8 Å for Ga, 2.4 Å for B; for 6H SiC: 7.7 and 6.1 Å for N, 4.0 and 3.9 Å for Al, 3.5 and 3.4 Å for Ga, 2.3 and 2.3 Å for B in HS and CS, respectively; for 15R SiC: 13.9 and 10.5 Å for N, 4.2 and 4.1 Å for Al, 3.6 and 3.5 Å for Ga, 2.4 and 2.3 Å for B in HS and CS, respectively.

[41] L. Patrick and W. J. Choyke, Phys. Rev. B 2, 2255 (1970).

[42] L. S. Aivazova, S. N. Gorin, V. G. Sidyakin, and I. M. Shvarts, Fiz. Tekh. Poluprovodn. 11, 1826 (1977) [Sov. Phys.—Semicond. 11, 1069 (1977)].

[43] L. S. Aivazova and Yu. M. Altaiskii, Fiz. Tekh. Poluprovodn. 12, 1453 (1978) [Sov. Phys.—Semicond. 12, 861 (1978)].

[44] H. B. Bebb and R. A. Chapman, J. Phys. Chem. Solids 28, 2087 (1967); H. B. Bebb, Phys. Rev. 185, 1116 (1969).

[45] R. C. Marshall, J. W. Faust, Jr., and C. E. Ryan,

Silicon Carbide—1973 (University of South Carolina Press, Columbia, 1974), p. 669.

[46] These values were obtained in the same way as Ref. 2 using the refractive index of 2*H* SiC reported by J. A. Powell, J. Opt. Soc. Am. 62, 341 (1972). The high-frequency dielectric constant in Ref. 2 was a little rough, and more accurate values were $\epsilon_\infty(\perp)=6.46$ and $\epsilon_\infty(\parallel)=6.79$.

[47] P. J. Dean, W. J. Choyke, and L. Patrick, J. Lumin. 15, 299 (1977).

[48] L. A. Hemstreet (private communication) kindly estimated the effective masses of 2*H* and 3*C* SiC by calculating the curvatures of the conduction-band minima of 2*H* and 3*C* SiC based on the data in Ref. 22.

[49] The values of E_{BX} were determined from the free-exciton luminescence and the bound-exciton luminescence of 3*C*, 4*H*, 6*H*, and 15*R* SiC (Ref. 27). These values are in good agreement with the data in the literatures; for 3*C*, for example, W. J. Choyke, D. R. Hamilton, and L. Patrick, Phys. Rev. 133, A1163 (1964); for 4*H*, Ref. 23; for 6*H*, W. J. Choyke and L. Patrick, Phys. Rev. 127, 1868 (1962); and for 15*R*, Ref. 26.

[50] J. R. Haynes, Phys. Rev. Lett. 4, 361 (1960).

[51] W. J. Choyke, D. R. Hamilton, and L. Patrick, Phys. Rev. 139, A1262 (1965).

[52] Yia-Chung Chang and T. C. McGill, Solid State Commun. 30, 187 (1979). In this paper results of many researchers were compared.

[53] R. R. Sharma and S. Rodriguez, Phys. Rev. 159, 649 (1967).